HHS Public Access

Author manuscript

J Chem Inf Model. Author manuscript; available in PMC 2018 November 27.

Published in final edited form as:

J Chem Inf Model. 2017 November 27; 57(11): 2833–2845. doi:10.1021/acs.jcim.7b00603.

Classical Molecular Dynamics with Mobile Protons

Themis Lazaridis[a,b,*] and **Gerhard Hummer**[c]

[a]Department of Chemistry, City College of New York/CUNY, 160 Convent Ave, New York, NY 10031, USA

[b]Graduate Programs in Chemistry, Biochemistry & Physics, Graduate Center, City University of New York, 365 Fifth Ave, New York, NY, 10016, USA

[c]Department of Theoretical Biophysics, Max Planck Institute of Biophysics, Max-von-Laue Str. 3, 60438 Frankfurt am Main, Germany

Abstract

An important limitation of standard classical molecular dynamics simulations is the inability to make or break chemical bonds. This restricts severely our ability to study processes that involve even the simplest of chemical reactions, the transfer of a proton. Existing approaches for allowing proton transfer in the context of classical mechanics are rather cumbersome and have not achieved widespread use and routine status. Here we reconsider the combination of molecular dynamics with periodic stochastic proton hops. To ensure computational efficiency, we propose a non-Boltzmann acceptance criterion that is heuristically adjusted to maintain the correct or desirable thermodynamic equilibria between different protonation states and proton transfer rates. Parameters are proposed for hydronium, Asp, Glu, and His. The algorithm is implemented in the program CHARMM and tested on proton diffusion in bulk water and carbon nanotubes, and on proton conductance in the gramicidin A channel. Using hopping parameters determined from proton diffusion in bulk water, the model reproduces the enhanced proton diffusivity in carbon nanotubes and gives a reasonable estimate of the proton conductance in gramicidin A.

Graphic Abstract

[*]Corresponding author. Tel. (212) 650-8364, tlazaridis@ccny.cuny.edu.

Supporting Information

Application of non-Boltzmann “threshold hopping” to 2-state model systems.

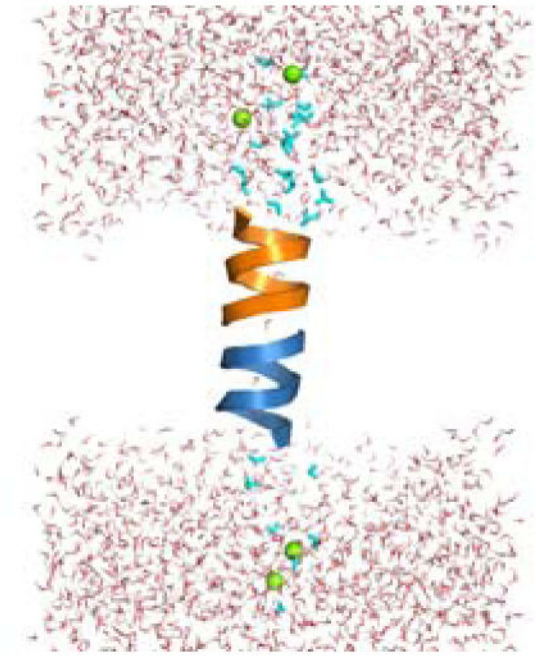

Keywords

molecular dynamics; proton transfer; proton conductance; pK_a; gramicidin; carbon nanotubes

INTRODUCTION

Chemical and biological systems are replete with mobile protons. Titratable residues in proteins can easily lose or gain protons upon modest changes in pH. Enzyme catalysis often involves proton transfer steps [1]. Nature's choice to temporarily store energy in electrochemical proton gradients ensured a prominent position of proton transport across biological membranes in systems such as proton channels [2], proton pumps [3,4], or proton-powered ATP synthases [5].

Most classical molecular dynamics simulations are based on empirical energy functions that do not allow chemical bonds to break or form. This, however, is crucial in proton mobility. Even proton diffusion in water cannot be properly treated without allowing for bond rearrangements. Diffusion of hydronium or hydroxide as intact ions ("vehicular diffusion") is much slower than the experimental diffusion rates. A large contribution to the diffusion of these species comes from the so called Grotthus mechanism ("structural diffusion"), whereby protons move by a succession of hops from hydronium or water to a neighboring water molecule or hydroxide, respectively [6,7].

Because of the need to make and break bonds, the obvious tool to treat proton transfer is quantum mechanics. The large size of biological systems usually necessitates the use of hybrid QM/MM methods[8–14]. Valuable information on proton and hydroxide transfer in bulk solution has been obtained from Car-Parrinello ab initio MD (CPMD) and path integral

methods [15–18]. In agreement with experiment [19,20], these studies showed that proton transfer in water is very fast, occurring on the fs-ps timescale. The mechanism involves breaking a hydrogen bond donated to the accepting water molecule (rate limiting step), formation of a Zundel ion, and reformation of an Eigen ion centered on the new hydronium [16,21]. For hydroxide a different mechanism was found whereby the stable 4-fold coordination of the O is transiently reduced to 3-fold, which is more conducive to proton transfer [17]. The substantial computational cost of these approaches has limited their application to small, bulk systems and short simulation times.

Computationally more efficient are semiempirical methods based on valence bond theory, primarily the Empirical Valence Bond (EVB) [22] and its multistate extension, MS-EVB [23,24]. In EVB the possible states of a moving proton comprise the diagonal elements of a Hamiltonian matrix and the off-diagonal coupling elements are fitted to experimental data or ab initio computations. Diagonalization of the Hamiltonian matrix produces a smooth adiabatic potential energy surface for proton transfer with forces computed based on the Hellman-Feynman theorem. The EVB formalism has been widely used for localized proton transfer in proteins [22]. MS-EVB appears to be best for transfer between water molecules, with only a handful of studies involving protein side chains [25,26]. With efficiency improvements, the computational cost has dropped to a factor of 2–5 over regular MD [27]. Multiple protons need special treatment, at additional computational cost [28]. Finally, an MS-EVB code is not a standard part of widely available software packages and this somewhat hinders its widespread application. An alternative to EVB is provided by classical dissociative models that view water as a collection of free H and O particles [29–34]. A more recent model utilizes explicit electron pairs [35,36]. These models have so far been applied mostly to pure water or materials science problems, with few applications to biological systems [37].

An attempt to allow proton hopping in classical MD simulations was made by Helms and coworkers with the Q-HOP algorithm [38], based on an earlier proposal [39]. In this method, a regular MD simulation is periodically interrupted by Monte Carlo steps attempting to move a titratable proton to a nearby atom. The hop is accepted or rejected based on probabilities calculated on the basis of independent quantum mechanical calculations, adjusted for the effect of the electrostatic environment. This algorithm is currently implemented in the NWCHEM package, but with limited documentation. Applications have included GFP [40], aquaporin [41], acetic acid titration in water [42], Fo-ATPase [43] and Nafion membranes [44]. Issues noted include the violation of detailed balance [45], and an inability to study multiple protons due to integration instabilities [44]. A similar algorithm that also violates detailed balance uses a set of six geometric and energetic criteria to accept a hop and performs a local structure adjustment after each hop [46]. A different approach that does satisfy detailed balance was proposed by Wolf & Graenhof [45,47]. The method is based on λ-dynamics [48] and thus has the shortcoming of unphysical intermediate λ values (a biasing potential is typically used to reduce the probability of such intermediate λ values). Thus far, it has been applied only to proton transfer between water molecules.

Proton transfer simulations bear some resemblance to constant pH simulations [49–52]. Both involve mobile protons in titratable sites, but in the latter the protons are in equilibrium with

an implicit reservoir, whereas in the former the protons move between explicit positions (the total number of protons in the system is conserved). In fact, in many constant pH algorithms no particles are added or removed, only the partial charges are changed. Constant pH simulations ignore the kinetics of changes in protonation state, i.e. they assume that a proton is always available and protonation/deprotonation is essentially instantaneous. This could conceivably give misleading results for the dynamics of the coupling of conformational and protonation state changes. Equilibrium protonation states in proteins are highly studied and benchmarked [53], but the kinetics of protonation state change has attracted much less attention.

The central idea of the algorithm proposed in this work is that of time scale separation: whereas the actual proton transfer from donor to acceptor is fast (~170 fs), committing to the transfer requires rate limiting solvent rearrangements in bulk water that are significantly slower (~1.7 ps) [54]. Assuming such a separation, we probe the fast proton transfer with instantaneous hops, and treat the Marcus-type solvent relaxation with classical dynamics. Although this separation of time scales is not as wide as in electron transfer, we argue it is sufficient for our purposes. The resulting algorithm is closest in spirit to Q-HOP, but uses a different acceptance criterion and addresses in more detail the timescale problem in water-amino acid side chain proton exchange. For the sake of computational efficiency, we forsake detailed balance and instead use heuristic rules inspired by model systems, designed to reproduce protonation equilibria and/or proton diffusion rates. The following section describes the algorithm and its implementation in CHARMM, followed by description of the computational Methods. The Results section presents tests in a number of model systems: proton diffusion in bulk water and in carbon nanotubes of different diameters, conductance in the gramicidin A ion channel, and amino acid side chain titration in bulk water.

ALGORITHM

Theoretical Framework

Consider a system containing a proton donor-acceptor pair in solution. To study proton transfer with a method such as CPMD, one would perform classical dynamics on a potential energy surface U(x) obtained from, say, density functional theory. Proton transfer would then amount to a continuous motion of the proton position from being in bonding distance to the donor to being in bonding distance to the acceptor.

Such proton transfer reactions have typical waiting times ~ 2 ps for water to water transfer and much longer for amino acid side chain to water transfer (see below). Moreover, the chemical part of the transfer, i.e., the breaking of the donor bond and the formation of the acceptor bond, is significantly faster (transition times ~ 200 fs). Since we are here not interested in the chemical part of the proton transfer dynamics, we use this separation of timescales to motivate an assumption of proton hopping dynamics. In such a model, proton transfer is described by discrete jumps between the two protonation states.

To formalize the proton hopping dynamics, we approximate the quantum mechanical energy surface by a combination of two diabatic energy surfaces, U_1 and U_2 [55]

$$U(x)=-\beta^{-1}\ln[e^{-\beta U1(x)}+e^{-\beta U2(x)}] \quad (1)$$

where $\beta = 1/k_BT$. In the case of DFT, the $U_i(x)$ could be obtained constructively, by restraining the proton distance to the donor or to the acceptor. An approximation obtained in such a way would be quite accurate everywhere, except in the transition region of proton transfer. In the context of classical simulations, the U_i correspond to classical molecular mechanics energy functions with the proton on the donor or on the acceptor.

The dynamics on the two surfaces amounts to a combination of free MD simulations, described by Liouville operators L_i for surface U_i, and jumps from points x on surface 1 to points f(x) on surface 2, and from y on surface 2 to g(y) on surface 1,

$$\frac{\partial p_1(x,t)}{\partial t}=L_1p_1(x,t)-k_{21}(x)p_1(x,t)+k_{12}(g^{-1}(x))p_2(g^{-1}(x),t) \quad (2)$$

$$\frac{\partial p_2(y,t)}{\partial t}=L_2p_2(y,t)+k_{21}(f^{-1}(y))p_1(f^{-1}(y),t)-k_{12}(y)p_2(y,t) \quad (3)$$

The mapping functions are used to conduct the “chemical” step of the proton transfer. However, finding maps f(x) and g(y) that allow the system to “tunnel” through the transition region is difficult in practice, and building these maps in a volume preserving and invertible form, g(f(x))=x and f(g(y))=y, is even more difficult. Moreover, the rates k_{ij} in these coupled Liouville equations would have to be chosen such that the Boltzmann distribution

$$p_i(x)=\exp(-\beta U_i(x))/\sum_j \int dy \exp(-\beta U_j(y)) \quad (4)$$

is recovered in the steady state, and that there are no net fluxes in the steady state because of microscopic time reversibility. In practice, this is difficult for several reasons, first because the use of mapping functions makes it difficult to formulate the flux-free condition, and second because in a Monte Carlo implementation with imperfect mapping functions, the acceptance rate of attempted hops would be very small.

To address this dual challenge, we take once more advantage of the time scale separation. We assume adiabaticity, i.e., that dynamics on each surface is sufficiently fast that we establish local equilibrium on each surface after a successful hop (this assumption is tested below). The dynamics is then reduced to Boltzmann sampling on each surface, and transitions between each surface with effective rates $\langle k_{12}(y)\rangle_2$ and $\langle k_{21}(x)\rangle_1$ averaged over the restricted Boltzmann distributions on each surface. These rates have to be constructed in

such a way that the equilibrium populations of states 1 and 2 are preserved, and the rate of transition between the two states is correct,

$$\int dx \exp(-\beta U_1(x)) / \int dy \exp(-\beta U_2(y)) = <k_{12}(y)>_2 / <k_{21}(x)>_1 \quad (5)$$

Here, we use the Metropolis criterion (in a time-discrete manner), modified by adjustable constants. We accept a hop from x on 1 to y=f(x) on 2 according to $\Delta U = U_2[f(x)] - U_1(x) - C$ in the Metropolis criterion, and from y on 2 to g(y) on 1 according to $\Delta U = U_1[g(y)] - U_2(y) - D$. Ideally, these maps would be chosen such that they transform candidate proton transfer reactant states into good proton transfer product states. By choosing the two constants C and D appropriately, we can satisfy both that states 1 and 2 have the correct relative equilibrium populations, and that the rates of transition between states 1 and 2 are correct. Therefore, if the adiabatic assumption is valid (namely that there is equilibration on each surface), we have recovered both proper Boltzmann sampling and correct rates.

In practice one should expect some issues. Most importantly, one has to be careful in mechanistic interpretations. The “dynamics” is certainly incorrect on the time scale of hopping. Nevertheless, it can be a good approximation if solvent fluctuations dominate the dynamics, as is assumed in Marcus theory of electron transfer. This seems to also be the case in proton transfer [56,57]. The solvent relaxation as a result of an accepted hop should be fast (to ensure rapid relaxation to the new state) and transitions should be relatively rare (to ensure proper sampling of the new surface). Care is also required when this type of algorithm is combined with accelerated sampling methods such as replica exchange that rely on exact sampling of the Boltzmann distribution [58].

Hop attempt and Acceptance Criterion

The simplest way to allow proton mobility in classical MD simulations is to intersperse discrete proton moves during a dynamics trajectory. That is, every certain number of MD steps an attempt is made to move a titratable proton to an eligible alternative location, i.e. a potential acceptor to which the titratable proton is hydrogen bonded. The key ingredient of the algorithm is then how the test configuration is constructed and the criterion by which it is accepted or rejected.

The molecular geometries and force field parameters of protonated and deprotonated species are usually different. For example, the bond lengths and bond angles in hydronium (see below) are slightly different from those in water. The same is true for protonated and deprotonated amino acid side chains. Thus, when a proton is moved, the geometry of the donor and acceptor species must be adjusted; otherwise, a large change in bonded energy may be incurred. For the same reason, the moving proton must be placed in a position consistent with the geometry of the protonated acceptor (e.g. for hydronium, it has to be placed in a roughly tetrahedral arrangement).

Even with these geometrical adjustments, the change in energy upon a proton hop will usually be very large because the solvent structure around the donor-acceptor pair is better

suited for the reactant state than the product state (the same effect is responsible for the activation barrier in condensed phase electron transfer reactions[59]). In reality, movement of the proton is slower than that of electrons, and a gradual adjustment of the solvation shell lowers the barrier. In stochastic hopping algorithms, however, the hop occurs instantaneously and the ΔE is too high (see Results section), leading to vanishing acceptance rates in standard Metropolis sampling.

One possible solution to this problem could be nonequilibrium switching moves [60,61], in which a brief nonequilibrium MD simulation is used to drive the proton from donor to acceptor and the move is accepted or rejected based on the work done. This approach is being pursued in constant pH simulations [62] but has substantial computational cost.

As described above, here we take an alternative approach ("threshold hopping") that is less rigorous but more computationally expedient. We use a modified Metropolis criterion where the test ΔE is replaced by ΔE-C, where C is an energy threshold chosen empirically. The algorithm clearly violates detailed balance, but attempts to correct for this violation by the appropriate choice of the energy thresholds. The Supporting Information explores the use of such thresholds in simple model systems and shows that an appropriate choice of the C parameters in the two directions can lead to the correct equilibrium distribution and dynamics. In its current form the algorithm does not conserve energy and is used with a thermostat, aiming to reproduce the canonical or isothermal-isobaric ensemble. A test of how well this is accomplished is given in Results. Energy conservation could possibly by enforced by local adjustments of the accepted product state. This issue will be investigated in future work.

Bond energies

Empirical (molecular mechanics, MM) energy functions are designed to reproduce relative energies of systems with the same atoms and bonds. The absolute values of MM energies are usually meaningless. When a bond is broken or formed, the change in energy reported by the force field does not include the energy of the bond itself. Thus, any scheme that involves changes in bonding must include these bond energies as an extra term (E_{be}). Whenever a hop is accepted, the bond energy of the donor is added and that of the acceptor is subtracted from this term. Experimental gas phase proton affinities give an initial estimate of these bond energy parameters (E_b) but their exact values are determined by the relative energies of the protonated and deprotonated forms in the energy function used.

Implementation in CHARMM

Implementation of the above algorithm requires changes in bonding during a dynamics trajectory, which most modeling packages are not designed to accommodate. In CHARMM, bonding information is contained in the protein structure file (PSF), which is assumed to be invariant during dynamics (except in certain free energy perturbation calculations where two versions of the PSF are used). It would be very disruptive to attempt changes in the lists of bonds and bond angles during an MD run. It is much easier, however, to make changes in the atom types and the partial charges. Thus, we opted to implement hopping by keeping the bonding lists the same and using dummy atoms for the disappearing protons. The dummy

atoms have 0 charge and no interactions of any type with their surroundings. They are used as placeholders for possible future protonation and they are kept together with their partner heavy atom using SHAKE constraints. Thus, the PSF must be generated with all potential protons present, i.e., all residues specified by the user as titratable should be fully protonated in the PSF.

Proton hopping is only allowed between hydrogen bonded molecules. A list of hydrogen bonds is maintained using the legacy HBOND facility in CHARMM (taking care to omit the relevant energy terms from the energy function). The user can specify the hydrogen bonding criteria (distance and angle) and also edit the donor and acceptor lists to restrict h-bond list generation only to titrating groups, cutting significantly the computational cost.

The excess proton is represented as classical hydronium (H3O) residues. A deprotonated H3O is identical to TIP3P but with an additional dummy atom. For each titratable residue, including hydronium, arrays are filled with the atom types and the partial charges of the protonated and deprotonated forms. For certain residues multiple deprotonated forms are included (e.g. the τ and π tautomers for His). The user selects the titratable residues and the starting protonation state of these residues.

The dummy atoms of each titratable residue are in specific locations, and this often necessitates switching the identity (position and velocity) of equivalent atoms. For example, the dummy atom in deprotonated H3O corresponds to H3. When H1 or H2 are considered for donation, they must be switched with H3. In protonated ASP the proton resides on OD2. If donation is considered to OD1, the identity of OD1 and OD2 are switched. The vast majority of water in a system will be standard, nontitratable TIP3P. If donation is considered to a TIP3P molecule, its identity will be switched with an H3O residue which has a place for an additional proton. The system must have enough H3O residues to allow the required proton transfers. Typically, 5 times as many H3O residues as the desired number of hydronium ions is sufficient.

The proton hop and the above identity switches must be done in a way that will not disrupt the integration of the equations of motion. Thus, not only the current coordinates and velocities must be switched, but also whatever arrays the code uses to propagate the state of the system. The results presented here used the CHARMM default leap frog integrator and may not necessarily work with other integrators. Upon proton hop acceptance, the velocity of the moving proton is set to zero. For computational efficiency, when the hop energy is calculated, the rest of the system is fixed. Only one hop is allowed per titratable residue per cycle (this can be revisited in the future). Hopping attempts are done sequentially with a random reversal of the order (both between and within residues) to avoid bias. However, introducing such a bias sometimes improves the results (see below). This issue will be explored in more detail in future work.

The algorithm was implemented into CHARMM as an additional module (MOBHY, which stands for “Mobile Hydrogen”). It includes two main subroutines, one called initially to set up the needed arrays and the initial protonation state of the titratable residues and one that is called during dynamics that performs the proton hop attempts.

METHODS

The solvation free energy of the classical hydronium model was calculated by Free Energy Perturbation [63], changing H_2O to H_3O^+, using the PERT module of CHARMM. This free energy plus the self-solvation free energy of TIP3P water (−6.10 kcal/mol [64]) gives the solvation free energy of the ion. These calculations were done in a box of 1000 water molecules using Particle Mesh Ewald. To relate this to the solvation free energy of the proton, we can imagine proton solvation taking place in three steps: evaporating a TIP3P water molecule ($\Delta G=-\Delta G^{solv}(H_2O)$), binding an H^+ to water in the gas phase ($\Delta G=-157.7$ kcal/mol from experiment [65]), and then inserting the H_3O^+ ion into water ($\Delta G=\Delta G^{solv}(H_3O^+)$, calculated as above). Thus, $\Delta G^{solv}(H^+) = \Delta G(H_2O->H_3O^+) -157.7$ kcal/mol.

The experimental solvation free energies are usually obtained from gas phase cluster studies and contain a contribution from the surface potential of water [66,67], which for TIP3P and monovalent ions is ±12.45 kcal/mol [68]. Our calculations are done with periodic boundary conditions and give the “intrinsic” solvation free energy, devoid of the surface potential contribution. Thus, to compare to experiment, this contribution must be subtracted. After these corrections, one obtains the intrinsic experimental value of −247 to −253 kcal/mol for the proton (or −95.6 to −101.6 kcal/mol for H_3O^+) [68,69].

The hopping algorithm was first tested in bulk water. A system of one ion in 982 water molecules was simulated. The system contained 5 H3O residues (1 true hydronium and 4 deprotonated ones, equivalent to TIP3P) and 978 TIP3P residues. The proton diffusion coefficient was calculated as follows: a 1-ns MD simulation was run at constant temperature (300.0 K) using the Hoover method [70] and a constant pressure of 1.0 bar using the Langevin piston method [71]. Particle Mesh Ewald was used for the long range electrostatic interactions [72]. Proton hops were attempted every 10 or 20 MD steps. The trajectory was “unwrapped” using the CHARMM MERGE command to remove effects of particle recentering due to periodic boundary conditions. Then a time series of the Cartesian coordinates of the hydronium O was created and $<r^2>$ was calculated for different time intervals, averaged over the time series, where r is the distance of the O from its original position. From a plot of $<r^2>$ vs. t, the slope of the initial linear region (with best statistics) was input into the Einstein relation $D=<r^2>/6t$ to obtain the diffusion coefficient D.

To calculate the electrophoretic mobility (velocity/electric field) a potential of 1 V was applied in the z direction over the entire cell length (~31Å). An MD simulation was run for 100 ps and the trajectory was unwrapped as above. The velocity of the H3O ion was calculated as the slope of the z coordinate vs. time plot. Each simulation was repeated three times with different random initial velocities.

To calculate pK_a values for amino acid side chains in water from populations of protonated and unprotonated forms one might intuitively attempt to use the definition of K_a, i.e. $[A^-][H^+]/[AH]$ and compute $[H^+]$ as a time average over the simulation ($1/V_{box}$ when the side chain is deprotonated and 0 otherwise) [42]. However, this is incorrect, for reasons explained

by De Jong et al. [73]. The $[H^+]$ in the above equation should be that of the deprotonated state, i.e. $1/V_{box}$, and not the time average.

The gramicidin A dimer (pdb id 1JNO [74]) was embedded and equilibrated in a DMPC membrane using the CHARMM-GUI web server [75]. The N-terminus was formylated and the C-terminus was ethanolaminated. For this system we used the charmm36 force field without CMAP; the latter causes problems with the D-amino acids [76]. With CMAP omitted, the dimer is very stable (backbone RMSD less than 1 Å in 1 ns). To speed-up ion translocation, the H3O ions were restrained in a cylinder of 5 Å radius above the opening of the channel. This restraint is equivalent to increasing the concentration of the ions.

Carbon nanotube coordinates were generated using a publicly available python script (http://chembytes.wikidot.com/buildcstruct). 2-loop "residues" of (6,6) and (11,11) carbon nanotubes were added to the charmm topology files, replication of which generated open-ended, unfunctionalized CNTs of arbitrary length. Here, we used tubes of 43 "residues", giving a length of about 100 Å. All atoms had zero partial charge and CHARMM atom type CA. The parameters for this atom type in the charmm36 force field were used. Water was placed inside the tube (45 in the narrow one, 639 in the wide one) and equilibrated. The waters were prevented from evaporating from the tube's ends using constraints from the MMFP module of charmm. Here constant temperature was maintained by scaling velocities every 10 steps if the average temperature deviates by more than 5 K (the Berendsen thermostat gave similar results). Diffusion coefficients were calculated with the one-dimensional version of the Einstein equation, $D=<r^2>/2t$.

RESULTS

Classical models for H_3O^+

In selecting a classical model we have two aims. First, to reproduce, as much as possible, the solvation configurations obtained by quantum mechanical methods and experiment. This is essential for preserving the mechanism of proton transfer. Second, because many potential applications involve movement through confined environments and desolvation makes an important contribution to the free energy barrier for such movements, it is also imperative to reproduce the aqueous solvation free energy.

A number of classical nonpolarizable models for hydronium have been proposed [39,45,77–79]. We tentatively chose the model proposed by Sagnella & Voth [77] with partial charges of −0.755 e on the O and +0.585 e on the H. The Lennard-Jones parameters were set equal to those of TIP3P water. A simulation of this model in water gave the expected configurations around H_3O^+, with three strong hydrogen bonds donated to water molecules and very weak h-bond acceptance. The solvation free energy of this model, however, was calculated to be −84.1 kcal/mol, somewhat lower than the reference value of −95.6 to −101.6 (see Methods). Scaling up the partial charges to −1.4 e for the O and +0.8 e for the H results in a solvation free energy −95.5 kcal/mol, which is at the edge of the target range. A recent study also found the need to increase the polarization of hydronium in order to reproduce the solvation free energy and activity derivatives of HCl solutions [80]. We will refer to the Sagnella-Voth model as svH3O and to the more polarized model as pH3O.

The oxygen-oxygen radial distribution functions for the two models are shown in Fig. 1. The svH3O model shows a peak of 5.5 at 2.6 Å and the pH3O shows a peak of 6.9 at 2.55 Å. CPMD simulations gave for the Eigen cation a peak of 4 at 2.6 Å[15] and MS-EVB3 a peak of 4.7 at 2.5 Å [81]. Experimenal neutron diffraction data of concentrated HCl solutions showed a peak of 4.7 at 2.5 Å [82]. However, because of the high HCl concentration, integration of the first peak in the experimental RDF gives 1.9 water oxygens, instead of 3. Thus, under dilute conditions, the peak should be higher; in fact, it could be as high as that of the pH3O model.

Proton Diffusion and Electrophoretic mobility in Bulk Water

In the case of H^+ diffusion in water, the free energy of the proton hopping reaction is zero. Thus, the energy threshold parameter (C) affects only the kinetics of the process. The kinetics is also influenced by other parameters of the algorithm, such as the number of time steps between attempted hops (IHOPFR) and possibly the criteria for deciding the presence of an h bond (RHB: distance between heavy atoms, AHB: OH…O angle). For the latter we found that variations within a reasonable range do not affect the hopping rates dramatically and used standard values (RHB=2.9Å for water, 3.1 Å for side chains in water, AHB=90°). This is consistent with the finding that proton transfer in water is limited by solvent preorganization and not by the chemical step [7].

Fig. 2 shows the distribution of energy changes upon proton hopping attempts in a simulation of 1 H_3O^+ in 982 water molecules with IHOPFR=10 and RHB=2.9 Å. In a total of 138721 attempts, only 851 were below 20 kcal/mol. Thus, for reasonable acceptance rates C should be above ~20 kcal/mol. The diffusion coefficient values obtained using different sets of parameters are listed in Table 1. The calculated diffusion coefficient is sensitive to the value of C, increasing with increasing C. For C=20 kcal/mol, the average over three independent 1-ns runs is 0.92 ± 0.2 $Å^2$/ps, close to the experimental value of 0.93 $Å^2$/ps [83]. A modest increase in IHOPFR does not change significantly the mean value, but increases the variability among duplicate runs. For comparison, the vehicular diffusion coefficient of hydronium (obtained by preventing proton hops) is 0.28 ± 0.05 $Å^2$/ps, similar to the self-diffusion coefficient of water (0.23 $Å^2$/ps [84].

With the values C=20 kcal/mol, IHOPFR=10 that give a good diffusion coefficient, the electrophoretic mobility is calculated to be 22.5 ± 5 $Å^2$/V ps (average of three runs), lower than the experimental value of 36.25 $Å^2$/V ps [85]. For the more polarized pH3O model, the higher hopping barriers required a larger C of 23.5 kcal/mol to reproduce the diffusion coefficient. The electrophoretic mobility of the pH3O model was 23 ± 4 $Å^2$/V ps.

Investigating the effect of proton hopping on the statistical thermodynamic properties of the hydronium-water system, we found that the probability distribution of the energy in a 1-ns simulation with IHOPFR=10 is indistinguishable from that without hopping (mean energy −9652 ± 47 kcal/mol in both cases). Thus, the hopping algorithm does not distort the sampling of the NPT ensemble. We also investigated the speed of energy relaxation after a successful hop in the same system. The average energy of the 3651 configurations that led to a successful hop tended to be higher than average (−9644 kcal/mol). In the first step after a hop it rose, on average, to −9629 kcal/mol and relaxed back to −9642 kcal/mol in about 6–7 steps. Thus, relaxation after a hop is quite fast, although, of course, not instantaneous.

It is of interest to compare the configurations that lead to a successful hop to those that do not. We examined the hydrogen bonding arrangement in 10 configurations of each type and found that in all configurations that led to a successful hop the accepting water molecule accepted only one hydrogen bond (from the hydronium), consistent with the "presolvation" concept and ab initio MD simulations [16,54]. Among the configurations that did not lead to a hop, in half of them the target water molecule accepted two hydrogen bonds (either both from the hydronium or one from the hydronium and one from another water molecule). In the remaining configurations the target water molecule accepted only one hydrogen bond. Thus, accepting one hydrogen bond appears to be a necessary but not sufficient condition for a successful hop. More detailed analysis and comparison with ab initio MD trajectories will be carried out in future work.

Carbon Nanotubes

Spatial confinement often affects water properties in dramatic ways [86,87]. Pristine carbon nanotubes are a completely hydrophobic model system that can serve as a limiting case for protein channels. Proton transport has been studied in CNTs using CPMD and the MS-EVB model [88]. The diffusion coefficient in narrow CNTs was found to be 17 $Å^2$/ps, compared to 0.4 for the same model in bulk water, an enhancement by a factor of over 40. An earlier study on smooth repulsive hydrophobic channels reported a one-order-of-magnitude increase in the proton diffusion constant in narrow channels relative to the bulk (4 vs. 0.45 $Å^2$/ps) [89]. The mechanism of proton transfer in CNTs was later investigated in detail [90]. Rasaiah and coworkers confirmed these results using a dissociable water model and obtained diffusion coefficients between 19 and 32 $Å^2$/ps for H^+ and 24 to 32 $Å^2$/ps for OH- [91]. Their results agreed with ab initio calculations in periodic systems [92], which, due to the presence of defects, exhibit much lower diffusion coefficients [88].

We examined proton hopping in two armchair CNTs, (6,6) and (11,11) with diameters of about 8 and 14.5 Å, respectively, and length of about 100 Å (Fig. 3). The narrow one allows only single file water occupancy. They were filled with water and constraints were placed to prevent the water from evaporating from the open edges. Five waters were replaced by H3O and one of them was designated as protonated.

Fig. 4 shows the distribution of proton hopping energies for svH3O in the two CNTs. The distribution in the wider CNT is similar to that in water, with a slightly lower minimum and slightly higher median (Min=3.35, Median=43). In the narrow CNT, however, the distribution is shifted significantly to lower values (Min=1.5, Median=21), consistent with a much faster PT.

We now examine what diffusion coefficient values we obtain if we use the C parameter determined in the bulk. In the wide CNT the 1-d diffusion coefficient (considering only translation along the tube) was calculated to be 1.4 $Å^2$/ps, slightly enhanced compared to bulk. In the narrow CNT acceptance rates are close to 100% and the one-dimensional diffusion coefficient is about 66 ± 25 $Å^2$/ps. This is in qualitative agreement with past studies but the extent of the enhancement seems excessive. One way that the diffusion coefficient could be reduced would be to give priority, while considering possible hops, to the proton that has just hopped, thus encouraging back transfers. This is achieved simply by

considering the three hydronium protons always in reverse order (H3,H2,H1). This scheme gives D=33±12 $Å^2$/ps, more in line with other theoretical estimates.

Proton conductance in gramicidin A

Gramicidin A is a 15-residue β-helical peptide with alternating L and D amino acids forming an ion channel upon head-to-head dimerization in membranes [93,94]. It has been extensively studied as the simplest model system of known structure for studying ion conduction, including protons. It has also been the subject of numerous computational studies [95–97]. No amino acid side chains are involved in proton transfer.

We used gramicidin A as the first biological testing ground of the proposed modeling approach (Fig. 5). The dimer (pdb id 1JNO) was inserted and equilibrated in a DMPC bilayer. 2 hydroniums and 2 Cl^- ions were placed on either side of the membrane, corresponding well with the typical experimental setup for measuring proton conductance (symmetric solutions of HCl)[98]. The Cl^- were free to move across periodic boundaries but not the hydroniums. The hydroniums were additionally restrained to move within a cylinder of 5 Å radius above the peptide. This corresponds to increasing the H^+ concentration to about 2 M. A voltage of 1.5 V was applied across the membrane and current was calculated from the number of H3O crossings and the time these crossings were observed. Conductance was calculated as current/voltage. For the svH3O model we obtained 2.4 nS and for the pH3O model 0.8 nS (average of three runs). The experimental conductance at 4 M is 0.53 nS for native gramicidin A [99] and 1 or 1.2 nS for covalently cross-linked gramicidin A [98]. Thus, the svH3O model overestimates conductance substantially, but the polarized one (with realistic solvation free energy) gives conductance very close to the experimental range. Of course, for a more precise estimate a much larger number of simulations is needed.

Protein side chains

In proton exchange between amino acid side chains and water one needs to consider not only kinetics but also thermodynamics. That is, the algorithm should reproduce experimental data on both the pK_a and the protonation/deprotonation rates. Examining these data, however, one realizes potential difficulties. Whereas the rate of protonation of carboxylates and imidazole is close to diffusion-limited, of the order 10^{10} –10^{11} $M^{-1}s^{-1}$, the rate of deprotonation is much lower, close to 10^6 s^{-1} for acetic acid and 10^3 s^{-1} for imidazolium [100]. The protonated forms of the side chains correspond to deep free energy wells, and getting out of these wells is very slow. This means that deprotonation would rarely if ever be observed in standard-length simulations [101]. Calculation of the equilibrium constant for His deprotonation in water by brute force MD based on population ratios would require multiple milliseconds of simulation. Similarly, the dynamics of proton relays through a His residue would be too slow to be observed directly in standard-length MD simulations. A possible strategy around this problem could be to use a modified His residue, referred to as “fast His” (or “fake His” if you will), with lower pK_a and higher deprotonation rate. The resulting time scales would then need to be corrected to account for this artificial acceleration.

The relative depth of the protonated and deprotonated minima is determined by the bond energy values, E_b. In the present algorithm only relative values are needed. To maintain some correspondence with gas phase data, the E_b for hydronium is fixed at the experimental gas phase value (165 kcal/mol [65]). Then, by varying the E_b value for the side chains we can shift the free energy difference between the protonated and deprotonated forms. An initial value for this parameter that gives a pK_a of ~ 1 is estimated by Free Energy Perturbation simulations in which the side chain is deprotonated and a water molecule is protonated. This value, together with the threshold parameters (C for deprotonation and D for protonation), is fine-tuned in MOBHY simulations that compute the equilibrium constant and the protonation and deprotonation rates. The final value of the E_b parameter that reproduces the experimental pK_a is obtained by using the relation $\Delta E_b = 2.3RT\Delta pK_a$. Both FEP and MOBHY simulations were done with a blocked amino acid in 186 water molecules (181 TIP3P and 5 H3O, concentration ~0.25M). A small box was purposely chosen to facilitate the convergence of the protonation state ratio calculation. The FEP calculation was repeated 5 times, each time converting a different H3O residue from water to hydronium. For the side chain work we used exclusively the svH3O model.

Glutamate

The experimental protonation (k_{on}) and deprotonation (k_{off}) rate constants of acetic acid are $4.5X10^{10}$ $M^{-1}s^{-1}$ and $7.8X10^{5}$ s^{-1}, respectively [100], which combine to give $K_a=k_{off}/k_{on}=1.7X10^{-5}$ M^{-1} and $pK_a=4.76$. For glutamate, $pK_a=4.3$, and if we assume k_{on} to be the same as for acetic acid, k_{off} is calculated to be $2.3X10^{6}$ s^{-1}.

The free energy of changing GluH to Glu and simultaneously one H_2O to H_3O^+ was calculated to be −145.7±1.6 kcal/mol. For a uniform distribution of the hydronium in the box, an entropic contribution of $RTlnN_{water}$=−3.1 kcal/mol should be added to this free energy to account for the distinguishability of the H_3O^+ vs. the indistinguishability of the H_2O molecules (or, equivalently, the translational entropy of the H_3O^+ in the box). In reality, the distribution is unlikely to be uniform (the hydronium is more likely to be close to Glu due to electrostatic attraction), so the above estimate is an upper limit. The experimental free energy of deprotonation is $\Delta G^o(1M) = 2.3RTpK_a = 5.84$ kcal/mol ($pK_a=4.3$), or $\Delta G^o(0.25M)= 5$ kcal/mol. If this is set equal to −145.7−(0 to 3.1) + E_b(GluH) − E_b(H3O), we obtain E_b(GluH)= 316 to 319 kcal/mol. For comparison, the gas phase proton affinity of Glu is 347.2 kcal/mol [65].

For the desired pK_a ~1 of a “fast” Glu (fGlu; same k_{on}, $k_{off}=4.5X10^{9}$ s^{-1}=1/220 ps), E_b should be reduced by 4.6 kcal/mol. Using E_b =312, the distribution of hopping energies from GluH to water has a minimum value of 20 and a median value of 54 kcal/mol. For protonation, the median value is 61 kcal/mol, but negative values are also observed. In simulations of deprotonated Glu and a hydronium, the hydronium is attracted electrostatically by the Glu and reaches it rapidly (within 20 ps) no matter its initial position in the box. It then remains in its vicinity, resulting in a great number of hopping attempts. The protonation rate constant is estimated from $1/\langle\tau_{on}\rangle = k_{on}[H^+]$, where $\langle\tau\rangle$ is the average time for protonation observed in the simulation. $[H^+]$ in our box is 0.246 M. With D=20 kcal/mol we obtain $\langle\tau_{on}\rangle$ ~ 98 ps, corresponding to k_{on} ~ $4X10^{10}$ $M^{-1}s^{-1}$

Deprotonation rates were estimated from a plot of the distance of the proton from the side chain (Fig. 6). The algorithm allows transient excursions of the proton to a neighboring water, but these "flickers" do not constitute true dissociation. True dissociation is here defined by two criteria: a) the proton gets to at least 5 Å away from the side chain, b) it stays away for at least 10 ps. These numerical values, admittedly somewhat arbitrary, were determined by visual examination of plots like that in Fig. 6. The wait times before true dissociation (τ) were averaged and used to make a rough estimate of the deprotonation rate ($k_{off} \sim 1/\langle\tau_{off}\rangle$). The value C=25 kcal/mol gave $k_{off} \sim 1/205$ ps and $pK_a = 1.1\pm0.4$ (average of 5 runs). Larger values of C give faster dissociation and lower pK_a values. Thus, the final parameters for fGlu are E_b=312, C=25, D=20.

To model real Glu, E_b should be shifted back up to 316. D should be decreased by the same amount to keep the same k_{on} and C should also be somewhat lowered, based on model system results presented in the SI. The exact extent of C lowering required is unclear, but the model studies suggest between 10 and 20%. Thus, we propose C=20 kcal/mol. Thus the parameters for real Glu are E_b=316, C=20, D=16. Verifying that these parameter values reproduce the experimental pK_a and k_{off} would require multimicrosecond simulations and is left for future work. Multiple 1-ns simulations show only transient flickers of the proton without true dissociation. But protonation is facile, on timescales consistent with the experimental k_{on}.

Aspartate

Because the Charmm36 energy difference between protonated and unprotonated forms is different for Glu and Asp, the E_b parameters for Asp and Glu have to be different as well. Free energy perturbation gave $^{-}133 \pm 1$ kcal/mol for the transformation GluH+ H_2O $^{-}$>Glu + H_3O^+. For pK_a=4, $\Delta G(0.25)$=4.6, which gives E_b = 303 to 306. For target pK_a~1, E_b should be shifted down to 299–302. Using E_b=299 with C=24 and D=20, we obtain pK_a=0.95±0.6. Thus these parameters are proposed for fAsp. For real Asp we propose E_b=303, C=20, D=16.

Histidine

Deprotonated His exists in two tautomeric forms, τ (or HSE, with the proton on NE1) and π (or HSD, with the proton on ND1). The relative population is τ:π ~ 4:1 [102], which corresponds to a free energy difference of 0.8 kcal/mol. An additional goal of modeling here is to roughly reproduce this experimental population ratio. Because the MM energies of the two tautomers in the Charmm force field are quite different, one needs to use different E_b parameters for each of them. Table 2 lists experimental and computational results used in the parameterization of His. As for Glu, free energy simulations were performed to compute the free energy of converting protonated His and water to deprotonated His and hydronium and these values were used to obtain initial values of E_b for the two His tautomers. Because deprotonated His is neutral, the distribution of H_3O^+ in the box is expected to be closer to uniform, so we included the full $RTlnN_w$ entropic term.

For a target pK_a of ~ 1 for "fast" His, the initial E_b values need to be shifted down to 245 and 263 kcal/mol. Protonation simulations starting from various initial positions for the

H_3O^+ and using D=30 kcal/mol give an average time to protonation $<\tau_{on}>$ ~ 360 ps, corresponding to a k_{on}~1.2X10^{10} $M^{-1}s^{-1}$, similar to experimental. However, the HSE/HSD ratio was systematically higher than 4. Raising E_b (HSE) to 264 and with C=22, D=30 we obtained pK_a= 0.84±1.0 and ratio HSE/HSD ~ 7.

For real His the E_b values should be shifted back up to E_b(HSD)= 253 and E_b(HSE)= 272 kcal/mol, D lowered to 22 kcal/mol and C lowered by ~ 20% to 18 kcal/mol. With these values protonation occurs readily but deprotonation does not occur at all in the timescale of 1 ns. Again, verifying that these values reproduce the experimental thermodynamics and kinetics of His protonation is not possible with current-length MD simulations.

CONCLUDING REMARKS

We present a new approach for incorporating proton mobility in classical MD simulations, with sufficient flexibility for large systems and multiple titratable sites. It bears a resemblance to previous efforts [38], but makes different choices in regard to the acceptance criterion and the parameterization. In addition, we present an in-depth discussion of the effect of these choices on thermodynamics and kinetics. Clearly, this approach is a phenomenological one, and does not address the mechanism of proton transfer, which can only be truly done by quantum mechanical methods. For many systems of biological or technological interest it could provide a fast initial picture that can be followed up with more rigorous but expensive methods. The computational overhead depends on the number of titratable protons for a given system size and the hopping frequency. For hop attempts every 10 steps and one titratable site in the systems considered here it is lowest (15%) for Glu/Asp with one proton, higher (35%) for His with two, and highest (50%) for H3O with three.

One serious problem in proton transfer processes that involve amino acid side chains is that the timescale of deprotonation is much longer than the duration of standard MD trajectories. Most theoretical approaches address this problem by computing free energy profiles and inferring dynamic properties based on rate theory [13,105]. This approach is elegant and rigorous, but does not provide a dynamic view in the way that a trajectory does. For example, in gramicidin A with the current approach one could directly observe how and on what time scale reorientation of the water wire takes place to conduct the next proton. In proton channels, such as M2 [105], one could directly observe the “shuttle” mechanism of proton conduction through a His ring. In proton conducting membrane proteins one could identify proton pathways in an unbiased way by placing hydroniums on either side and applying voltage. The present algorithm could capture such dynamic effects in regard to proton hopping events, as long as the kinetics of side chain deprotonation is treated properly. Additional timescale issues arising from slow conformational changes will have to be treated by standard enhanced sampling methods such as hyperdynamics [106] or metadynamics [107]. However, one needs to be careful as to how these disparate processes may be coupled.

One important question regarding the present algorithm is the transferability of the empirical parameters. Our intent has been to determine these parameters from simulations in bulk water and then use them unchanged under different environments, as was done in this article with the carbon nanotubes and gramicidin A. Otherwise, the method would not have any

predictive power. The results so far are encouraging, but more tests in biological systems are needed to verify that the parameters are indeed transferable.

The proposed algorithm, like previous efforts [38,46], does not satisfy detailed balance in regard to the proton hopping steps. It should be noted in this regard that detailed balance is sufficient but not necessary for achieving Boltzmann sampling [108,109]. In fact, recent work has shown that violation of detailed balance can lead to better performance [110–112]. However, a weaker, “balance” condition is necessary to guarantee Boltzman sampling. This condition requires that the transition matrix leaves the Boltzman distribution invariant. The present algorithm, like some constant pH MD algorithms [113,114], cannot formally guarantee that. It tries to achieve proper sampling (and dynamics) in an average sense by empirically manipulating the transition rates between the protonation states. Finding a way to perform the proton hops observing the balance condition would allow us to remove much of the empiricism and ensure that the method will work properly under any condition. One possibility to explore is the novel nonequilibrium moves already implemented in constant pH simulations. [62]

The parameterization of the remaining titratable amino acids and hydroxide will be reported in the near future. Another possibility for future extension is concerted transfers through hydroxylated amino acids such as Ser, Thr, or Tyr. It would also be of interest to conduct a detailed comparison with ab initio MD trajectories to seek correlations in the configurations that allow a proton hop in the two approaches.

Supplementary Material

Refer to Web version on PubMed Central for supplementary material.

Acknowledgments

TL is supported by the NSF (MCB 1244207) and NIH (RO1 GM117146). GH is supported by the Max Planck Society. This work was carried out in part during TL’s sabbatical year at the Max Planck Institute for Biophysics, Frankfurt, Germany, during which he was also supported in part by that institution. Martin Vögele is acknowledged for help with carbon nanotube modeling and Marilyn Gunner for comments on the manuscript. Infrastructure support was provided in part by RCMI grant 5G12MD007603 from the National Institutes of Health.

References

1. Klinman JP. The Role of Tunneling in Enzyme Catalysis of C-H Activation. Biochim Biophys Acta - Bioenerg. 2006; 1757:981–987.
2. Decoursey TE. The Voltage-Gated Proton Channel: A Riddle, Wrapped in a Mystery, inside an Enigma. Biochemistry. 2015; 54:3250–3268. [PubMed: 25964989]
3. Wraight CA. Chance and Design-Proton Transfer in Water, Channels and Bioenergetic Proteins. Biochim Biophys Acta - Bioenerg. 2006; 1757:886–912.
4. Wikström M, Sharma V, Kaila VRI, Hosler JP, Hummer G. New Perspectives on Proton Pumping in Cellular Respiration. Chem Rev. 2015; 115:2196–2221. [PubMed: 25694135]
5. Fillingame RH, Jiang W, Dmitriev OY, Jones PC. Structural Interpretations of F0 Rotary Function in the Escherichia Coli F1F0 ATP Synthase. Biochim Biophys Acta. 2000; 1458:387–403. [PubMed: 10838053]
6. Cukierman S. Et Tu, Grotthuss! And Other Unfinished Stories. Biochim Biophys Acta - Bioenerg. 2006; 1757:876–885.

7. Agmon N, Bakker HJ, Campen RK, Henchman RH, Pohl P, Roke S, Thamer M, Hassanali A. Protons and Hydroxide Ions in Aqueous Systems. Chem Rev. 2016; 116:7642–7672. [PubMed: 27314430]
8. Berendsen HJC, Mavri J. Quantum Simulation of Reaction Dynamics by Density Matrix Evolution. J Phys Chem. 1993; 97:13464–13468.
9. Bała P, Grochowski P, Lesyng B, McCammon JA. Quantum-Classical Molecular Dynamics Simulations of Proton Transfer Processes in Molecular Complexes and in Enzymes. J Phys Chem. 1996; 100:2535–2545.
10. Sharafeddin OA, Hinsen K, Carrington T, Roux B. Mixing Quantum-Classical Molecular Dynamics Methods Applied to Intramolecular Proton Transfer in Acetylacetone. J Comput Chem. 1997; 18:1760–1772.
11. Billeter SR, Van Gunsteren WF. Computer Simulation of Proton Transfers of Small Acids in Water. J Phys Chem A. 2000; 104:3276–3286.
12. Kaila VRI, Wikström M, Hummer G. Electrostatics, Hydration, and Proton Transfer Dynamics in the Membrane Domain of Respiratory Complex I. Proc Natl Acad Sci U S A. 2014; 111:6988–6993. [PubMed: 24778264]
13. Dong H, Fiorin G, Degrado WF, Klein ML. Proton Release from the Histidine-Tetrad in the M2 Channel of the Influenza A Virus. J Phys Chem B. 2014; 118:12644–12651. [PubMed: 25317959]
14. Lammers S, Lutz S, Meuwly M. Reactive Force Fields for Proton Transfer Dynamics. J Comput Chem. 2008; 29:1048–1063. [PubMed: 18072179]
15. Tuckerman M, Laasonen K, Sprik M, Parrinello M. Ab-Initio Molecular-Dynamics Simulation of the Solvation and Transport of Hydronium and Hydroxyl Ions in Water. J Chem Phys. 1995; 103:150–161.
16. Marx D. Proton Transfer 200 Years after Von Grotthuss: Insights from Ab Initio Simulations. ChemPhysChem. 2006; 7:1849–1870.
17. Marx D, Chandra A, Tuckerman ME. Aqueous Basic Solutions: Hydroxide Solvation, Structural Diffusion, and Comparison to the Hydrated Proton. Chem Rev. 2010; 110:2174–2216. [PubMed: 20170203]
18. Hassanali, Aa, Cuny, J., Verdolino, V., Parrinello, M. Aqueous Solutions: State of the Art in Ab Initio Molecular Dynamics. Philos Trans A Math Phys Eng Sci. 2014; 372:20120482. [PubMed: 24516179]
19. Luz Z, Meiboom S. The Activation Energies of Proton Transfer Reactions in Water. J Am Chem Soc. 1964; 86:4768–4769.
20. Woutersen S, Bakker HJ. Ultrafast Vibrational and Structural Dynamics of the Proton in Liquid Water. Phys Rev Lett. 2006; 96:5–8.
21. Markovitch O, Chen H, Izvekov S, Paesani F, Voth Ga, Agmon N. Special Pair Dance and Partner Selection: Elementary Steps in Proton Transport in Liquid Water. J Phys Chem B. 2008; 112:9456–9466. [PubMed: 18630857]
22. Warshel, A. Computer Modeling of Chemical Reactions in Enzymes and Solutions. Wiley; 1991.
23. Voth GA. Computer Simulation of Proton Solvation and Transport in Aqueous and Biomolecular Systems. Acc Chem Res. 2006; 39:143–150. [PubMed: 16489734]
24. Knight C, Voth GA. The Curious Case of the Hydrated Proton. Acc Chem Res. 2012; 45:101–109. [PubMed: 21859071]
25. Maupin CM, Wong KF, Soudackov AV, Kim S, Voth GA. A Multistate Empirical Valence Bond Description of Protonatable Amino Acids. J Phys Chem A. 2006; 110:631–639. [PubMed: 16405335]
26. Maupin CM, Castillo N, Taraphder S, Tu C, McKenna R, Silverman DN, Voth GA. Chemical Rescue of Enzymes: Proton Transfer in Mutants of Human Carbonic Anhydrase II. J Am Chem Soc. 2011; 133:6223–6234. [PubMed: 21452838]
27. Yamashita T, Peng Y, Knight C, Voth GA. Computationally Efficient Multiconfigurational Reactive Molecular Dynamics. J Chem Theory Comput. 2012
28. Wang F, Voth GA. A Linear-Scaling Self-Consistent Generalization of the Multistate Empirical Valence Bond Method for Multiple Excess Protons in Aqueous Systems. J Chem Phys. 2005; 122:1–9.

29. Stillinger FH, David CW. Polarization Model for Water and Its Ionic Dissociation Products. J Chem Phys. 1978; 69:1473.
30. Weber TA, Stillinger FH. Dynamical Study of the H5O2+ + H3O2− Neutralization Reaction Using the Polarization Model. J Chem Phys. 1982; 77:4150.
31. Ojamae L, Shavitt I, Singer SJ. Potential Models for Simulations of the Solvated Proton in Water. J Chem Phys. 1998; 109:5547–5564.
32. Lussetti E, Pastore G, Smargiassi E. A Fully Polarizable and Dissociable Potential for Water. Chem Phys Lett. 2003; 381:287–291.
33. Mahadevan TS, Garofalini SH. Dissociative Water Potential for Molecular Dynamics Simulations. J Phys Chem B. 2007; 111:8919–8927. [PubMed: 17604393]
34. van Duin, ACTV., Chenyu, Z., Kaushik, J., Vyascheslav, B., Goddard, WA. A Reaxff Reactive Force-Field for Proton Transfer Reactions in Bulk Water and Its Applications to Heterogeneous Catalysis. In: Asthagiri, A., Janik, MJ., editors. Computational Catalysis. 2013. p. 223-276.
35. Kale S, Herzfeld J. Proton Defect Solvation and Dynamics in Aqueous Acid and Base. Angew Chemie - Int Ed. 2012; 51:11029–11032.
36. Bai C, Herzfeld J. Surface Propensities of the Self-Ions of Water. ACS Cent Sci. 2016; 2:225–231. [PubMed: 27163053]
37. Pomès R, Roux B. Molecular Mechanism of H+ Conduction in the Single-File Water Chain of the Gramicidin Channel. Biophys J. 2002; 82:2304–2316. [PubMed: 11964221]
38. Lill MA, Helms V. Molecular Dynamics Simulation of Proton Transport with Quantum Mechanically Derived Proton Hopping Rates (Q-HOP MD). J Chem Phys. 2001; 115:7993–8005.
39. Schmid RG, Brickmann J. Molecular Dynamics Simulation of the Proton Transport in Water. Ber Bunsenges Phys Chem. 1997; 101:1816–1827.
40. Lill MA, Helms V. Proton Shuttle in Green Fluorescent Protein Studied by Dynamic Simulations. Proc Natl Acad Sci U S A. 2002; 99:2778–2781. [PubMed: 11880630]
41. De Groot BL, Frigato T, Helms V, Grubmuller H. The Mechanism of Proton Exclusion in the Aquaporin-1 Water Channel. J Mol Biol. 2003; 333:279–293. [PubMed: 14529616]
42. Gu W, Frigato T, Straatsma TP, Helms V. Dynamic Protonation Equilibrium of Solvated Acetic Acid. Angew Chemie - Int Ed. 2007; 46:2939–2943.
43. Gu W, Helms V. Tightly Connected Water Wires Facilitate Fast Proton Uptake at the Proton Entrance of Proton Pumping Proteins. J Am Chem Soc. 2009; 131:2080–2081. [PubMed: 19159297]
44. Devanathan R, Venkatnathan A, Rousseau R, Dupuis M, Frigato T, Gu W, Helms V. Atomistic Simulation of Water Percolation and Proton Hopping in Nafion Fuel Cell Membrane. J Phys Chem B. 2010; 114:13681–13690. [PubMed: 20860379]
45. Wolf MG, Groenhof G. Explicit Proton Transfer in Classical Molecular Dynamics Simulations. J Comput Chem. 2014; 35:657–671. [PubMed: 24497402]
46. Selvan ME, Keffer DJ, Cui S, Paddison SJ. A Reactive Molecular Dynamics Algorithm for Proton Transport in Aqueous Systems. J Phys Chem C. 2010; 114:11965–11976.
47. Wolf MG, Grubmuller H, Groenhof G. Anomalous Surface Diffusion of Protons on Lipid Membranes. Biophys J. 2014; 107:76–87. [PubMed: 24988343]
48. Kong X, Brooks CL III. λ-Dynamics: A New Approach to Free Energy Calculations. J Chem Phys. 1996; 105:2414–2423.
49. Chen W, Morrow BH, Shi C, Shen JK. Recent Development and Application of Constant pH Molecular Dynamics. Mol Simul. 2014; 40:830–838. [PubMed: 25309035]
50. Lee J, Miller BT, Damjanovic A, Brooks BR. Constant pH Molecular Dynamics in Explicit Solvent with Enveloping Distribution Sampling and Hamiltonian Exchange. J Chem Theory Comput. 2014; 10:2738–2750. [PubMed: 25061443]
51. Goh GB, Laricheva EN, Brooks CL. Uncovering pH-Dependent Transient States of Proteins with Buried Ionizable Residues. J Am Chem Soc. 2014; 136:8496–8499. [PubMed: 24842060]
52. Donnini S, Ullmann RT, Groenhof G, Grubmüller H. Charge-Neutral Constant pH Molecular Dynamics Simulations Using a Parsimonious Proton Buffer. J Chem Theory Comput. 2016; 12:1040–1051. [PubMed: 26881315]

53. Nielsen JE, Gunner MR, Garcia-Moreno EB. The pK a Cooperative: A Collaborative Effort to Advance Structure-Based Calculations of pK a Values and Electrostatic Effects in Proteins. Proteins Struct Funct Bioinforma. 2011; 79:3249–3259.
54. Berkelbach TC, Lee HS, Tuckerman ME. Concerted Hydrogen-Bond Dynamics in the Transport Mechanism of the Hydrated Proton: A First-Principles Molecular Dynamics Study. Phys Rev Lett. 2009; 103:3–6.
55. Zheng W, Brooks BR, Hummer G. Protein Conformational Transitions Explored by Mixed Elastic Network Models. Proteins Struct Funct Bioinforma. 2007; 69:43–57.
56. Tuckerman M, Laasonen K, Sprik M, Parrinello M. Ab Initio Molecular Dynamics Simulation of the Solvation and Transport of H3O+ and OH− Ions in Water. J Phys Chem. 1995; 99:5749–5752.
57. Day TJF, Schmitt UW, Voth GA. The Mechanism of Hydrated Proton Transport in Water. J Am Chem Soc. 2000; 122:12027–12028.
58. Rosta E, Buchete NV, Hummer G. Thermostat Artifacts in Replica Exchange Molecular Dynamics Simulations. J Chem Theory Comput. 2009; 5:1393–1399. [PubMed: 20046980]
59. Marcus RA. Electron Transfer Reactions in Chemistry: Theory and Experiment. Angew Chem Int Ed. 1993; 32:1111–1222.
60. Nilmeier JP, Crooks GE, Minh DDL, Chodera JD. Nonequilibrium Candidate Monte Carlo Is an Efficient Tool for Equilibrium Simulation. Proc Natl Acad Sci U S A. 2011; 108:E1009–18. [PubMed: 22025687]
61. Chen Y, Roux; B. Efficient Hybrid Non-Equilibrium Molecular Dynamics - Monte Carlo. J Chem Phys. 2014:114107.
62. Chen Y, Roux B. Constant-pH Hybrid Nonequilibrium Molecular Dynamics–Monte Carlo Simulation Method. J Chem Theory Comput. 2015; 11:3919–3931. [PubMed: 26300709]
63. Chipot, C., Pohorille, A., editors. Free Energy Calculations. Springer; 2007.
64. Shirts MR, Pande VS. Solvation Free Energies of Amino Acid Side Chain Analogs for Common Molecular Mechanics Water Models. J Chem Phys. 2005; 122:134508. [PubMed: 15847482]
65. Moser A, Range K, York DM. Accurate Proton Affinity and Gas-Phase Basicity Values for Molecules Important in Biocatalysis. J Phys Chem B. 2010; 114:13911–13921. [PubMed: 20942500]
66. Hummer G, Pratt LR, Garcia aE, Berne BJ, Rick SW. Electrostatic Potentials and Free Energies of Solvation of Polar and Charged Molecules. J Phys Chem B. 1997; 101:3017–3020.
67. Darden T, Pearlman D, Pedersen LG. Ionic Charging Free Energies: Spherical versus Periodic Boundary Conditions. J Chem Phys. 1998; 109:10921–10935.
68. Lamoureux G, Roux B. Absolute Hydration Free Energy Scale for Alkali and Halide Ions Established from Simulations with a Polarizable Force Field. J Phys Chem B. 2006; 110:3308–3322. [PubMed: 16494345]
69. Grossfield A, Ren P, Ponder JW. Ion Solvation Thermodynamics from Simulations with a Polarizable Force Field. J Am Chem Soc. 2003; 125:15671–15682. [PubMed: 14664617]
70. Hoover WG. Canonical Dynamics: Equilibrium Phase-Space Distributions. Phys Rev A. 1985; 31:1695–1697.
71. Feller SE, Zhang YH, Pastor RW, Brooks BR. Constant-Pressure Molecular-Dynamics Simulation - the Langevin Piston Method. J Chem Phys. 1995; 103:4613–4621.
72. Darden T, York D, Pedersen L. Particle Mesh Ewald: An NlogN Method for Ewald Sums in Large Systems. J Chem Phys. 1993; 98:10089–10092.
73. De Jong DH, Schafer LV, de Vries AH, Marrink SJ, Grubmuller H, Berendsen HJC. Determining Equilibrium Constants for Dimerization Reactions from Molecular Dynamics Simulations. J Comput Chem. 2011; 32:1919–1928. [PubMed: 21469160]
74. Townsley LE, Tucker Wa, Sham S, Hinton JF. Structures of Gramicidins A, B, and C Incorporated into Sodium Dodecyl Sulfate Micelles. Biochemistry. 2001; 40:11676–11686. [PubMed: 11570868]
75. Jo S, Kim T, Iyer VG, Im W. CHARMM-GUI: A Web-Based Graphical User Interface for CHARMM. J Comput Chem. 2008; 29:1859–1865. [PubMed: 18351591]

76. Ingolfsson HI, Li Y, Vostrikov VV, Gu H, Hinton JF, Koeppe RE, Roux B, Andersen OS. Gramicidin A Backbone and Side Chain Dynamics Evaluated by Molecular Dynamics Simulations and Nuclear Magnetic Resonance Experiments. I: Molecular Dynamics Simulations. J Phys Chem B. 2011; 115:7417–7426. [PubMed: 21574563]
77. Sagnella DE, Voth GA. Structure and Dynamics of Hydronium in the Ion Channel Gramicidin A. Biophys J. 2011; 70:2043–2051.
78. Kusaka I, Wang Z, Seinfeld JH. Binary Nucleation of Sulfuric Acid-Water: Monte Carlo Simulation Binary Nucleation of Sulfuric Acid-Water: Monte Carlo Simulation. J Chem Phys. 1998; 108:6829–6848.
79. Jang SS, Molinero V, Tahir C, Goddard WAI. Nanophase-Segregation and Transport in Nafion 117 from Molecular Dynamics Simulations: Effect of Monomeric Sequence. J Phys Chem B. 2004; 108:3149–3157.
80. Bonthuis DJ, Mamatkulov SI, Netz RR. Optimization of Classical Nonpolarizable Force Fields for OH− and H3O+ J Chem Phys. 2016; 144:1–10.
81. Wu Y, Chen H, Wang F, Paesani F, Voth GA. An Improved Multistate Empirical Valence Bond Model for Aqueous Proton Solvation and Transport. J Phys Chem B. 2008; 112:467–482. [PubMed: 17999484]
82. Botti A, Bruni F, Imberti S, Ricci MA, Soper AK. Ions in Water: The Microscopic Structure of a Concentrated HCl Solution. J Chem Phys. 2004; 121:7840–7848. [PubMed: 15485246]
83. Hille, B. Ionic Channels in Excitable Membranes. 2. Sinauer; 1991.
84. Wang JH, Robinson CV, Edelman IS. Self-Diffusion and Structure of Liquid Water III. J Am Chem Soc. 1953; 75:466–470.
85. Duso AB, Chen DDY. Proton and Hydroxide Ion Mobility in Capillary Electrophoresis. Anal Chem. 2002; 74:2938–2942. [PubMed: 12141650]
86. Rasaiah JC, Garde S, Hummer G. Water in Nonpolar Confinement: From Nanotubes to Proteins and Beyond. Annu Rev Phys Chem. 2008; 59:713–740. [PubMed: 18092942]
87. Köfinger J, Hummer G, Dellago C. Single-File Water in Nanopores. Phys Chem Chem Phys. 2011; 13:15403–15417. [PubMed: 21779552]
88. Dellago C, Naor MM, Hummer G. Proton Transport through Water-Filled Carbon Nanotubes. Phys Rev Lett. 2003; 90:105902. [PubMed: 12689010]
89. Brewer ML, Schmitt UW, Voth GA. The Formation and Dynamics of Proton Wires in Channel Environments. Biophys J. 2001; 80:1691–1702. [PubMed: 11259283]
90. Cao Z, Peng Y, Yan T, Li S, Li A, Voth GA. Mechanism of Fast Proton Transport along One-Dimensional Water Chains Confined in Carbon Nanotubes. J Am Chem Soc. 2010; 132:11395–11397. [PubMed: 20669967]
91. Lee SH, Rasaiah JC. Proton Transfer and the Diffusion of H+ and OH-Ions along Water Wires. J Chem Phys. 2013; 139:124507. [PubMed: 24089786]
92. Bankura A, Chandra A. Hydroxide Ion Can Move Faster than an Excess Proton through One-Dimensional Water Chains in Hydrophobic Narrow Pores. J Phys Chem B. 2012; 116:9744–9757. [PubMed: 22793519]
93. Andersen OS. Gramicidin Channels. Ann Rev Physiol. 1984; 46:531–548. [PubMed: 6201133]
94. Andersen OS, Koeppe RE. Molecular Determinants of Channel Function. Physiol Rev. 1992; 72:S89–S158. [PubMed: 1279736]
95. Roux B. Computational Studies of the Gramicidin Channel Computational Studies of the Gramicidin Channel. Acc Chem Res. 2002; 35:366–375. [PubMed: 12069621]
96. Braun-Sand S, Burykin A, Chu ZT, Warshel A. Realistic Simulations of Proton Transport along the Gramicidin Channel: Demonstrating the Importance of Solvation Effects. J Phys Chem B. 2005; 109:583–592. [PubMed: 16851050]
97. Qin Z, Tepper HL, Voth GA. Effect of Membrane Environment on Proton Permeation through Gramicidin a Channels. J Phys Chem B. 2007; 111:9931–9939. [PubMed: 17672487]
98. Cukierman S. Proton Mobilities in Water and in Different Stereoisomers of Covalently Linked Gramicidin A Channels. Biophys J. 2000; 78:1825–1834. [PubMed: 10733963]

99. Akeson M, Deamer DW. Proton Conductance by the Gramicidin Water Wire. Model for Proton Conductance in the F1F0 ATPases? Biophys J. 1991; 60:101–109. [PubMed: 1715764]

100. Eigen M, Kruse W, Maass G, De Maeyer L. Rate Constants of Protolytic Reactions in Aqueous Solution. Prog Rxn Kinet. 1964; 2:287–318.

101. Park JM, Laio A, Iannuzzi M, Parrinello M. Dissociation Mechanism of Acetic Acid in Water. J Am Chem Soc. 2006; 128:11318–11319. [PubMed: 16939231]

102. Reynolds WF, Peat IR, Freedman MH, Lyerla JJR. Determination of the Tautomeric Form of the Imidazole Ring of L-Histidine in Basic Solution by Carbon-13 Magnetic Resonance Spectroscopy. J Am Chem Soc. 1973; 95:328–331. [PubMed: 4687673]

103. Tanokura M. 1H-NMR Study on the Tautomerism of the Imidazole Ring of Histidine Residues I. Microscopic Pk Values and Molar Ratios of Tautomers in Histidine-Containing Peptides. Biochim Biophys Acta. 1983; 742:576–585. [PubMed: 6838890]

104. Ralph EK, Grunwald E. Kinetics of Proton Exchange in the Ionization and Acid Dissociation of Imidazole in Aqueous Acid. J Am Chem Soc. 1969; 91:2422–2425.

105. Liang R, Swanson JMJ, Madsen JJ, Hong M, DeGrado WF, Voth GA. Acid Activation Mechanism of the Influenza A M2 Proton Channel. Proc Natl Acad Sci. 2016; 112:E6955–E6964.

106. Voter AF. Hyperdynamics: Accelerated Molecular Dynamics of Infrequent Events. Phys Rev Lett. 1997; 78:3908–3911.

107. Laio A, Parrinello M. Escaping Free-Energy Minima. Proc Natl Acad Sci U S A. 2002; 99:12562–12566. [PubMed: 12271136]

108. Manousiouthakis VI, Deem MW. Strict Detailed Balance Is Unnecessary in Monte Carlo Simulation. J Chem Phys. 1999; 110:2753–2756.

109. Frenkel D. Speed-up of Monte Carlo Simulations by Sampling of Rejected States. Proc Natl Acad Sci. 2017; 101:17571–17575.

110. Ichiki A, Ohzeki M. Violation of Detailed Balance Accelerates Relaxation. Phys Rev E. 2013; 88:20101.

111. Sakai Y, Hukushima K. Eigenvalue Analysis of an Irreversible Random Walk with Skew Detailed Balance Conditions. Phys Rev E. 2016; 93:43318.

112. Takahashi K, Ohzeki M. Conflict between Fastest Relaxation of a Markov Process and Detailed Balance Condition. Phys Rev E. 2016; 93:12129.

113. Baptista AM, Teixeira VH, Soares CM. Constant-pH Molecular Dynamics Using Stochastic Titration. J Chem Phys. 2002; 117:4184–4200.

114. Swails JM, York DM, Roitberg AE. Constant pH Replica Exchange Molecular Dynamics in Explicit Solvent Using Discrete Protonation States: Implementation, Testing, and Validation. J Chem Theory Comput. 2014; 10:1341–1352. [PubMed: 24803862]

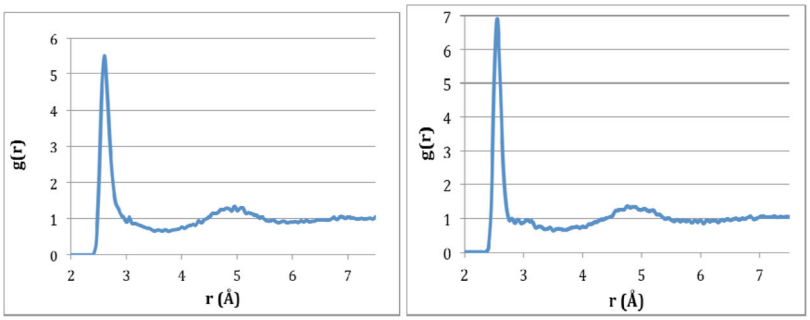

Fig. 1.
Hydronium O-water O radial distribution functions for svH3O (left) and pH3O (right).

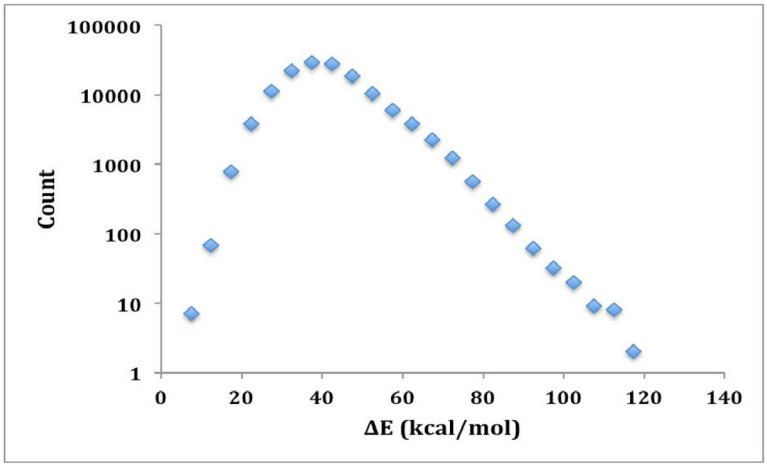

Fig. 2.

Distribution of energy changes upon hopping attempts for svH3O in bulk water (C=0, no hops accepted). The lowest value is 7.8 and the median value 40 kcal/mol.

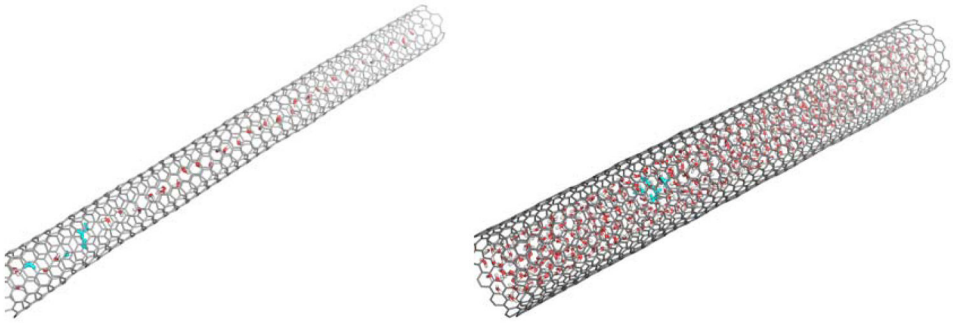

Fig. 3.
Carbon nanotubes studied with diameter 8 Å (left) and 14.5 Å (right). The H3O residues are shown in cyan, only one of which is a real hydronium.

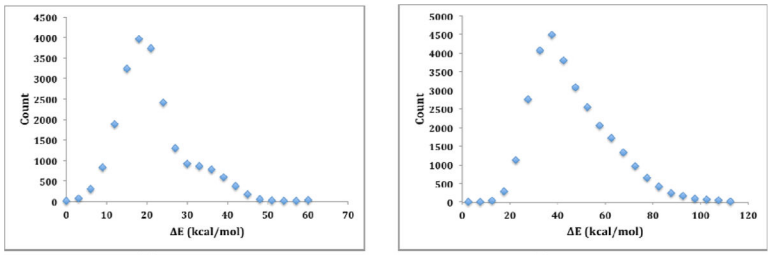

(a) (b)

Fig. 4.

Distribution of proton hopping energies in the (6,6) carbon nanotube (a) and the (11,11) carbon nanotube (b).

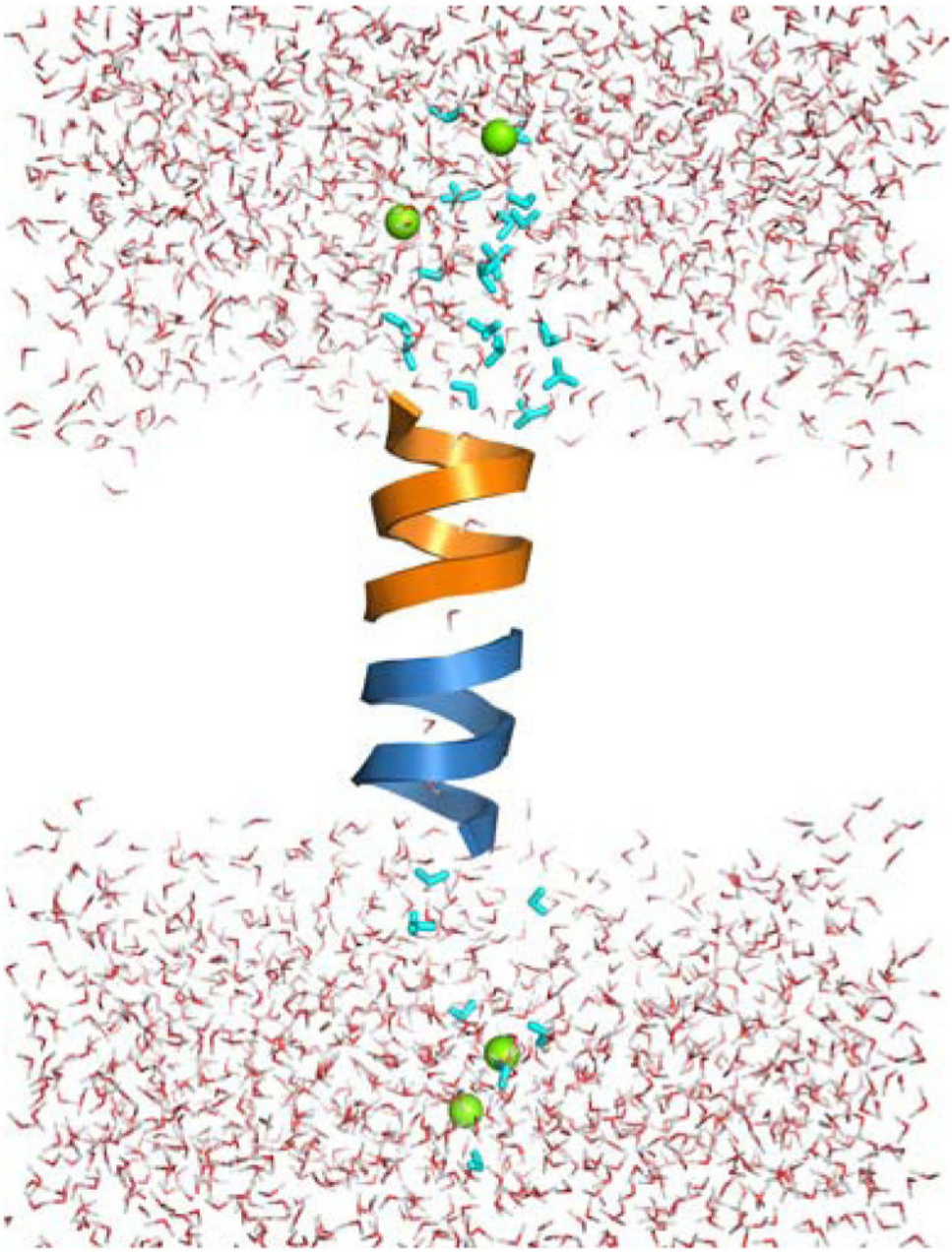

Fig. 5.

The gramicidin A dimer in DMPC lipid membrane (not shown for clarity). Chloride ions are shown in green and the H3O residues in cyan. Only four of them are real hydroniums, two on each side of the membrane.

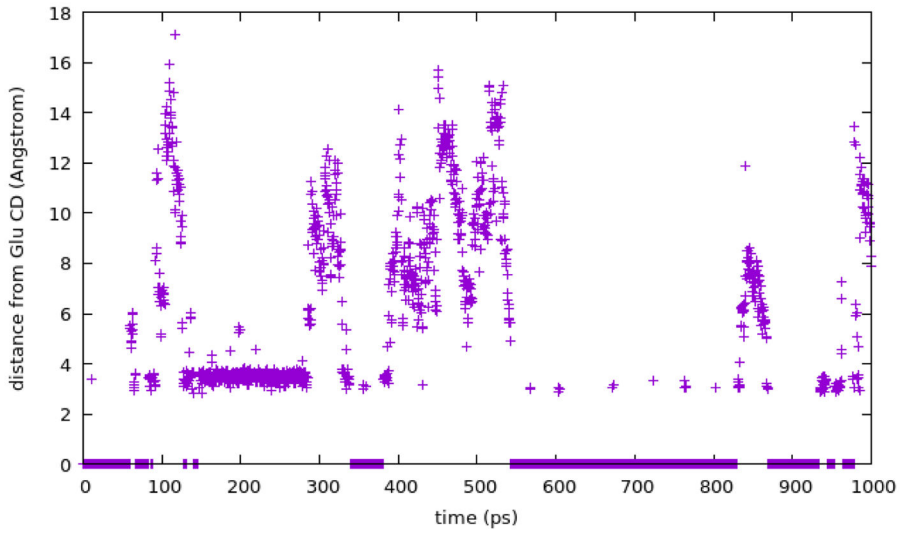

Fig. 6.

Proton distance from Glu CD atom, used to calculate the deprotonation rate. (E_b =312, C=25, D=20)

Table 1

H^+ diffusion coefficient for different threshold values for the svH3O model (averages of 3–5 runs). The experimental value is 0.93 $Å^2$/ps [83].

C (kcal/mol)	IHOPFR	D ($Å^2$/ps)
-	-	0.28 ± 0.05
19	10	0.50 ± 0.02
20	10	0.92 ± 0.2
20	20	0.92 ± 0.3
21	10	1.41 ± 0.2

Table 2

Experimental and computational results for the two tautomers of His. Free energy and E_b values are in kcal/mol.

	HSD	HSE	Ref/Note
pK_a	6.73	6.12	[103]
k_{on} ($M^{-1}s^{-1}$)	1.8 X10^{10}	1.8 X10^{10}	*a*
k_{off} (s^{-1})	3.4 X10^{3}	1.4 X10^{4}	*a*
ΔG^o(1M)	9.1	8.3	*b*
ΔG^o(0.25M)	8.3	7.5	*c*
ΔG(comp)	−76.7 ± 1.6	−95.8 ± 1	*d*
E_b (initial)	253	271	*e*
E_b (fHis)	245	263	*f*
E_b (His,final)	253	272	*g*

*a*Derived from the values for imidazole [104], assuming that k_{on} is the same and calculating k_{off} from k_{on} and the pK_a values

bΔG^o(1M)= 2.3RTpK_a at 298K

cΔG^o(0.25M)= ΔG^o(1M)+RTln(0.25)

*d*Computed free energy of converting protonated His and water to deprotonated His and hydronium

*e*From ΔG^o(0.25M)= ΔG(comp)−RTlnN_w+E_b−E_b(H3O).

For comparison, the gas phase proton affinity of 4-methyl-imidazolium is 227.7 kcal/mol [65]

*f*From E_b(initial)−2.3RT(6.5-1)

*g*From E_b(fHis)+2.3RT(6.5-1)